GEOPHYSICAL RESEARCH LETTERS, VOL. 37, L12202, doi:10.1029/2010GL043646, 2010

Click Here for Full Article

An improved parameterization of wind-blown sand flux on Mars that includes the effect of hysteresis

Jasper F. Kok[1]

Received 20 April 2010; accepted 19 May 2010; published 25 June 2010.

[1] Saltation, the wind-driven hopping motion of sand grains, forms dunes and ripples, and ejects fine dust particles into the atmosphere on Mars. Although the wind speed at which saltation is initiated, the "fluid threshold," has been studied extensively, the wind speed at which saltation is halted, the "impact threshold," has been poorly quantified for Mars conditions. I present an analytical model of the impact threshold, which is in agreement with measurements and numerical simulations for Earth conditions. For Mars conditions, the impact threshold is approximately an order of magnitude below the fluid threshold, in agreement with previous studies. Saltation on Mars can thus be sustained at wind speeds an order of magnitude less than required to initiate it, leading to the occurrence of hysteresis. I include the effect of hysteresis into an improved parameterization of sand transport on Mars. **Citation:** Kok, J. F. (2010), An improved parameterization of wind-blown sand flux on Mars that includes the effect of hysteresis, *Geophys. Res. Lett.*, *37*, L12202, doi:10.1029/2010GL043646.

1. Introduction

[2] Saltation, the wind-driven hopping motion of sand grains, forms dunes and ripples [*Bagnold*, 1941], and ejects fine dust into the atmosphere of Mars, which greatly affects its climate [*Leovy*, 2001]. Moreover, electric fields generated in saltation and dust storms [*Kok and Renno*, 2008] could affect atmospheric chemistry [*Kok and Renno*, 2009a] and produce electric discharges [*Ruf et al.*, 2009].

[3] Saltation is initiated when the wind shear velocity (defined as $u^* = \sqrt{\tau/\rho_a}$, where τ is the wind shear stress and ρ_a the air density) exceeds the "fluid threshold" at which surface particles are lifted [*Bagnold*, 1941]. Once initiated, saltation is maintained by the ejection ("splashing") of surface particles by impacting saltating particles [*Kok and Renno*, 2009b]. This process transfers momentum to the soil bed more efficiently than fluid drag does, and thus allows saltation to be sustained below the fluid threshold. The lowest shear velocity at which saltation can be sustained in this manner is termed the "impact threshold" [*Bagnold*, 1941]. For loose sand on Earth, the ratio of the impact and fluid thresholds is approximately 0.82 [*Bagnold*, 1937]. No measurements of the impact threshold for Mars conditions exist, but the numerical study of *Kok* [2010] found the Martian impact threshold to be approximately an order of magnitude below the fluid threshold. The earlier studies of *Claudin and Andreotti* [2006] and *Almeida et al.* [2008] also found the Martian impact threshold to be substantially below the fluid threshold.

[4] The small ratio of the impact and fluid thresholds on Mars allows saltation there to occur for wind speeds well below the fluid threshold [*Kok*, 2010]. Indeed, once saltation is initiated by a localized wind gust, it will continue downwind until the wind speed drops below the impact threshold. The occurrence of saltation at instantaneous wind speeds between the impact and fluid thresholds thus depends on the history of the system [*Kok*, 2010], a phenomenon known as "hysteresis."

[5] The effect of hysteresis can be roughly quantified by considering that the probability that saltation takes place is the sum of (i) the probability that the wind speed exceeds the fluid threshold, and (ii) the probability that the wind speed is between the impact and the fluid thresholds, multiplied by the probability that saltation was initiated more recently than that it was halted [*Kok*, 2010]. By using a Weibull distribution to describe the probability function of the instantaneous wind speed as a function of the average wind speed [*Wu and Chiu*, 1983; *Seguro and Lambert*, 2000], which in turn depends on the average shear velocity, *Kok* [2010] obtained an approximate expression for the probability that saltation transport takes place at any given moment:

$$P_{\mathrm{tr}} = \exp\left\{-\left[\frac{u^*_{\mathrm{ft}}\Gamma(1+1/k)}{\overline{u^*}}\right]^k\right\} + \exp\left\{-\left[\frac{u^*_{\mathrm{ft}}\Gamma(1+1/k)}{\overline{u^*}}\right]^k\right\} \times \frac{\exp\left\{-\left[\frac{u^*_{\mathrm{it}}\Gamma(1+1/k)}{\overline{u^*}}\right]^k\right\} - \exp\left\{-\left[\frac{u^*_{\mathrm{ft}}\Gamma(1+1/k)}{\overline{u^*}}\right]^k\right\}}{1 - \exp\left\{-\left[\frac{u^*_{\mathrm{it}}\Gamma(1+1/k)}{\overline{u^*}}\right]^k\right\} + \exp\left\{-\left[\frac{u^*_{\mathrm{ft}}\Gamma(1+1/k)}{\overline{u^*}}\right]^k\right\}}, \quad (1)$$

where Γ is the gamma function, k is the shape factor of the Weibull distribution, u^*_{it} and u^*_{ft} are the impact and fluid thresholds, and $\overline{u^*}$ is the average shear velocity. Depending on the application, $\overline{u^*}$ can for example be the monthly, daily, or hourly-averaged shear velocity [*Wu and Chiu*, 1983], as long as the distribution of wind speeds over the respective time periods follows a Weibull distribution, and the shape factor k is appropriately adjusted [*Kok*, 2010].

[6] In order to use equation (1) to calculate sand transport on Mars, the impact threshold must be quantified. Although the numerical study of *Kok* [2010] quantified the impact threshold for a particular surface pressure and temperature, the high computational cost makes this method difficult to use in determining the impact threshold for the wide range of thermodynamic conditions occurring on Mars [*Leovy*,

[1]Advanced Study Program, National Center for Atmospheric Research, Boulder, Colorado, USA.

0094-8276/10/2010GL043646

2001]. Here, I therefore develop an analytical model capable of calculating the impact threshold for a wide range of thermodynamic conditions.

[7] The results of the analytical model for Earth conditions are in agreement with measurements [*Bagnold*, 1937] and the numerical results of *Kok and Renno* [2009b]. For Mars conditions, the impact threshold is approximately an order of magnitude below the fluid threshold, and consistent with the numerical result of *Kok* [2010]. I use the analytical model to obtain an empirical expression of the impact threshold for use in future studies, and also derive an improved parameterization of the saltation mass flux that includes the effect of hysteresis.

2. Analytical Model of the Impact Threshold

[8] I start the analytical derivation of the impact threshold by considering the typical trajectory of a sand particle of size D_p saltating over a bed of similar particles. The trajectory of the particle is determined mainly by gravity and fluid drag, and I thus neglect secondary forces due to particle spin, electrostatics, turbulence, and interparticle collisions [*Kok and Renno*, 2008, 2009b]. Since the particle concentration in steady-state saltation stays constant, this typical trajectory must yield an average impact speed that is as likely to result in the loss of the saltating particle to the soil bed, as it is to splash up a second particle [*Kok and Renno*, 2009b]. Below, we use this condition to calculate the value of the impact threshold on Earth and Mars.

[9] Since particles strike the soil at angles of only ~5–15° from horizontal [*Rice et al.*, 1995], the vertical component of the impact speed is much smaller than the horizontal component. The horizontal speed gained by the particle over its trajectory can thus be expressed as

$$\overline{\Delta v_x} = \overline{v_{imp}} - \overline{v_{x0}} = \frac{\overline{\overline{F_{D,x}}}\,\overline{t_{hop}}}{m}, \tag{2}$$

where $\overline{v_{imp}}$ and $\overline{v_{x0}}$ are the impact and horizontal lift-off speeds averaged over the ensemble of saltating particles, $\overline{t_{hop}}$ is the ensemble-averaged hop duration, and m is the particle mass. The trajectory-averaged drag force in the horizontal direction ($\overline{\overline{F_{D,x}}}$), which has a double overbar to represent the average over the trajectory of the ‘average’ saltating particle, can be approximated as [*Anderson and Haff*, 1991]

$$\overline{\overline{F_{D,x}}} \approx \frac{\pi D_p^2}{8}\rho_a \overline{\overline{C_D}}\left(\overline{\overline{U_x}} - \overline{\overline{v_x}}\right)\overline{\overline{v_R}}, \tag{3}$$

where $\overline{\overline{v_x}}$ and $\overline{\overline{U_x}}$ are respectively the trajectory-averaged horizontal particle speed and wind speed, for which I derive approximate expressions below. Since the vertical particle speed is generally much smaller than the difference between the wind speed and the horizontal particle speed [*Bagnold*, 1941], a reasonable approximation of the average relative speed $\overline{\overline{v_R}}$ between the particle and the wind is

$$\overline{\overline{v_R}} = \left|\overline{\overline{U_x}} - \overline{\overline{v_x}}\right|. \tag{4}$$

Furthermore, the average drag coefficient $\overline{\overline{C_D}}$ for irregularly-shaped sand particles is approximately given by [*Kok and Renno*, 2009b]

$$\overline{\overline{C_D}} = \left[\left(\frac{32}{\overline{\overline{Re}}}\right)^{2/3} + 1\right]^{3/2}, \tag{5}$$

where $\overline{\overline{Re}} = \rho_a D_p \overline{\overline{v_R}}/\mu$ is the average particle Reynolds number, with the viscosity μ given by the Sutherland relation

$$\mu = \mu_0\left[\frac{T_0 + c}{T + c}\right](T/T_0)^{3/2}. \tag{6}$$

For the Martian atmosphere, which is predominantly CO_2 [*Leovy*, 2001], we have $c = 240$ K and $\mu_0 = 1.48 \times 10^{-5}$ kg/m s at $T_0 = 293.15$ K [*Crane Company*, 1988].

[10] The average horizontal wind speed $\overline{\overline{U_x}}$ depends on the wind profile at the impact threshold. Since the particle concentration approaches zero near the impact threshold, the wind profile is unperturbed from that in the absence of saltation. The average wind speed experienced by a saltating particle over its trajectory can thus be approximated from the logarithmic “law of the wall” for turbulent flow over an aerodynamically rough surface [*Bagnold*, 1941]:

$$\overline{\overline{U_x}} = \frac{u_{it}^*}{\kappa}\ln\left(\frac{\overline{\overline{z}}}{z_0}\right), \tag{7}$$

where $\kappa = 0.40$ is the von Kármán constant, $\overline{\overline{z}}$ is the average height of the particle above the surface during its hop, and $z_0 = D_p/30$ is the aerodynamic roughness length of a flat bed of sand particles. Inserting equations (3)–(7) into equation (2) then yields

$$u_{it}^* = \frac{\kappa}{\ln(\overline{\overline{z}}/z_0)}\left[\overline{\overline{v_x}} + \sqrt{\frac{\overline{v_{imp}} - \overline{v_{x0}}}{C\overline{t_{hop}}}}\right], \tag{8}$$

where $C = 3\rho_a \overline{\overline{C_D}}/(4\rho_p D_p)$.

[11] The impact threshold thus depends on the average horizontal lift-off ($\overline{v_{x0}}$) and impact ($\overline{v_{imp}}$) speeds, the duration of the “average” saltation hop ($\overline{t_{hop}}$), and the mean height ($\overline{\overline{z}}$) and horizontal particle speed ($\overline{\overline{v_x}}$) of the “average” saltation trajectory. I derive approximate expressions for these quantities in the subsequent sections.

2.1. Average Particle Speed at Impact and Lift-Off

[12] I approximate the average particle speed at impact and lift-off by using that the number of splashed particles (N_{spl}) must balance the number of saltating particles lost to the soil bed (N_{loss}) at steady state [*Kok and Renno*, 2009b]. These quantities can be approximated by [*Anderson and Haff*, 1991; *Kok and Renno*, 2009b]

$$N_{spl} = \sum_i \frac{a}{\sqrt{g_{eff} D_p}} v_{imp}^i, \tag{9a}$$

$$N_{loss} = \sum_i 1 - P_{reb}\left(v_{imp}^i\right), \tag{9b}$$

where i sums over all saltating particles that impact the soil surface per unit time and unit area, and g_{eff} is the effective

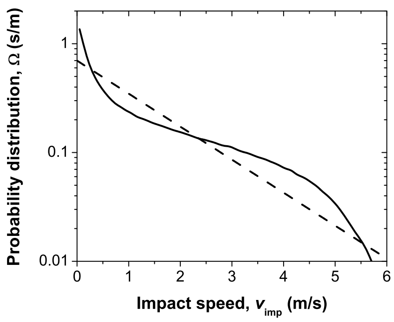

Figure 1. Simulations with the numerical saltation model COMSALT (solid line [*Kok and Renno*, 2009b]) of the probability distribution of the impact speed of 250 μm saltating particles for Earth conditions at $u^* = 0.5$ m/s. The dashed black line denotes the approximate exponential distribution (equation (12)) corresponding to the simulated mean impact speed $\overline{v_{imp}}$.

particle acceleration due to both gravity and the vertical component of the cohesive force on soil particles (see Text S1 of the auxiliary material).[1] I take the probability P_{reb} that a saltating particle will rebound as [*Anderson and Haff*, 1991]

$$P_{reb} = B\left[1 - \exp(-\gamma v_{imp})\right]. \quad (10)$$

The parameter values $a = 0.020$, $B = 0.96$, and $\gamma = 1$ s/m were determined by the numerical study of *Kok and Renno* [2009b] and are consistent with laboratory and numerical experiments [e.g., *Anderson and Haff*, 1991; *Rice et al.*, 1995].

[13] In steady state, we have that $N_{spl} = N_{loss}$, and thus

$$\sum_i \frac{a}{\sqrt{g_{eff} D_p}} v^i_{imp} = \sum_i 1 - B\left[1 - \exp\left(-\gamma v^i_{imp}\right)\right]. \quad (11)$$

I solve equation (11) for the ensemble-averaged impact speed $\overline{v_{imp}}$ by assuming a plausible distribution of the impact speed. Simulations with the numerical saltation model COMSALT [*Kok and Renno*, 2009b] indicate that the impact speed is approximately exponentially distributed (see Figure 1), and I thus assume

$$\Omega(v_{imp}) = \frac{\exp\left(-v_{imp}/\overline{v_{imp}}\right)}{\overline{v_{imp}}}, \quad (12)$$

where $\Omega(v_{imp})$ is the probability density function of the impact speed. Combining equations (11) and (12) and solving for $\overline{v_{imp}}$ then yields

$$\overline{v_{imp}} = \frac{(1-B)\sqrt{g_{eff}D_p}}{2a} - \frac{1}{2\gamma} + \sqrt{\frac{1}{4\gamma^2} + \left(\frac{1-B}{2a}\right)^2 g_{eff}D_p + \frac{(1+B)\sqrt{g_{eff}D_p}}{2a\gamma}}. \quad (13)$$

Equation (13) indicates that $\overline{v_{imp}}$ is not dependent on the shear velocity [*Kok and Renno*, 2009b], which was indeed confirmed by recent wind-tunnel measurements [*Rasmussen and Sørensen*, 2008; *Creyssels et al.*, 2009]. Moreover, equation (13) yields $\overline{v_{imp}} \approx 1.2$ m/s for 250 μm particles on Earth, which is in good agreement with those measurements [*Kok*, 2010].

[14] In addition to the average impact speed, we also need to approximate the average lift-off speed. Particles can lift-off from the surface either as splash ejecta or as rebounds following a surface collision. The average lift-off speed is thus the sum of two components:

$$\overline{v_{lift}} = \int_0^\infty P_{reb}(v_{imp})\Omega(v_{imp})\overline{\alpha_R} v_{imp} dv_{imp} + f_{ej}\overline{v_{ej}}, \quad (14)$$

where $\overline{\alpha_R} \approx 0.55$ [*Rice et al.*, 1995] is the average fraction of momentum retained by a particle upon colliding with the soil surface, and f_{ej} is the fraction of particles lifting off from the surface that are splash ejecta. I obtain this fraction by combining equations (9a), (11), and (12), which yields $f_{ej} = a\overline{v_{imp}}/\sqrt{g_{eff}D}$. Furthermore, the average ejected particle speed $\overline{v_{ej}}$ was derived in Section 2.2 of *Kok and Renno* [2009b] and approximately equals

$$\overline{v_{ej}} = \frac{\overline{\alpha_{ej}}\sqrt{g_{eff}D}}{a}\left[1 - \exp\left(-\frac{\overline{v_{imp}}}{40\sqrt{g_{eff}D}}\right)\right], \quad (15)$$

where $\overline{\alpha_{ej}} = \overline{\alpha_{ej,0}}\sqrt{g/g_{eff}}$ (see Text S1), and where $\overline{\alpha_{ej,0}} \approx 0.15$ is the average fraction of impacting momentum that is contained in the splash ejecta for collisions of cohesionless sand [*Rice et al.*, 1995]. Substituting equation (15) into equation (14) and evaluating the integral yields

$$\overline{v_{lift}} = B\overline{\alpha_R}\,\overline{v_{imp}}\left[1 - \frac{1}{\left(1+\gamma\overline{v_{imp}}\right)^2}\right] + \frac{a\overline{v_{imp}}}{\sqrt{g_{eff}D}}\overline{v_{ej}}. \quad (16)$$

The average horizontal and vertical lift-off speeds are then

$$\overline{v_{x0}} = \overline{v_{lift}}\cos\overline{\theta_{lift}};\ \overline{v_{z0}} = \overline{v_{lift}}\sin\overline{\theta_{lift}}, \quad (17)$$

where $\overline{\theta_{lift}} \approx 40°$ is the average lift-off angle [*Anderson and Haff*, 1991; *Rice et al.*, 1995].

2.2. Average Hop Time and Particle Height

[15] I derive expressions for the average hop time and particle height from the equation of motion in the vertical direction,

$$\frac{dv_z}{dt} = \frac{F_{D,z}}{m} - g \approx -\frac{3\rho_a\overline{\overline{C_D}}}{4\rho_p D_p} v_z\overline{\overline{v_R}} - g = -\frac{v_z}{\tau_r} - g, \quad (18)$$

where $F_{D,z}$ is the drag force in the vertical direction, and the relaxation time $\tau_r = (C\overline{\overline{v_R}})^{-1}$ determines how quickly the

[1] Auxiliary materials are available in the HTML. doi:10.1029/2010GL043646.

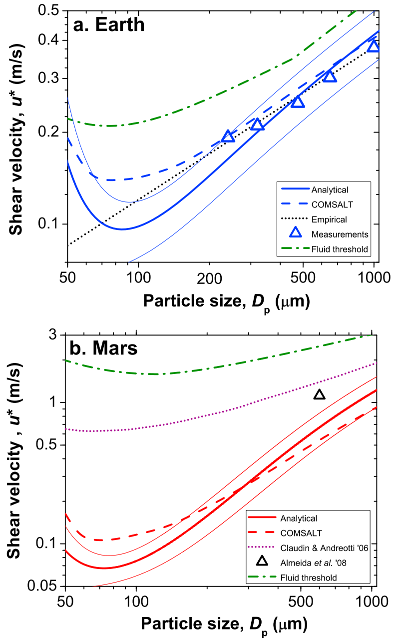

Figure 2. (a) Analytical calculation of the Earth impact threshold (thick blue line) and its uncertainty (thin blue lines (see Text S2 for details)). Plotted for comparison are measurements (triangles [*Bagnold*, 1937; *Iversen and Rasmussen*, 1994]), Bagnold's empirical relation (dotted black line [*Bagnold*, 1937]), the numerical result with COMSALT (dashed blue line, as by *Kok and Renno* [2009b], except that results account for cohesive forces on soil particles following Text S1), and the fluid threshold (dash-dotted green line [*Greeley and Iversen*, 1985]). (b) Analytical calculation of the Mars impact threshold (thick red line) and its uncertainty (thin red lines (see Text S2 for details)). Plotted for comparison are numerical and analytical calculations of the impact threshold with COMSALT (dashed red line, as by *Kok* [2010], except that results account for cohesive forces on soil particles following Text S1); dotted purple line, by *Claudin and Andreotti* [2006]; and triangle, by *Almeida et al.* [2008]). Also plotted is the fluid threshold (dash-dotted green line [*Greeley and Iversen*, 1985]).

particle speed approaches the fluid speed. The solution to equation (18) is

$$v_z = (\overline{v_{z0}} + g\tau_r)\exp(-t/\tau_r) - g\tau_r. \quad (19)$$

I now obtain the average hop duration $\overline{t_{hop}}$ by integrating equation (19) over time to obtain z and solving for the time where $z = 0$, which yields the recursive formula

$$\overline{t_{hop}} = \left(\frac{\overline{v_{z0}}}{g} + \tau_r\right)\left[1 - \exp\left(-\overline{t_{hop}}/\tau_r\right)\right]. \quad (20)$$

Additionally, I approximate the average particle height as $\overline{\overline{z}} = \overline{z_{max}}/2$, where I obtain the maximum trajectory height $\overline{z_{max}}$ by solving for the time t where $v_z = 0$ in equation (19) and substituting that into the expression for z, which yields

$$\overline{z_{max}} = \overline{v_{z0}}\tau_r - g\tau_r^2 \ln\left(1 + \frac{\overline{v_{z0}}}{g\tau_r}\right). \quad (21)$$

2.3. Average Horizontal Particle Speed

[16] I derive the average horizontal particle speed $\overline{\overline{v_x}}$ from the horizontal equation of motion (see equations (3) and (4)),

$$\frac{dv_x}{dt} = -C\left(v_x - \overline{\overline{U_x}}\right)\left|v_x - \overline{\overline{U_x}}\right|, \quad (22)$$

solving for v_x by using that $\overline{\overline{U_x}} > v_x$ yields

$$v_x = \frac{Ct\overline{\overline{U_x}}\left(\overline{\overline{U_x}} - \overline{v_{x0}}\right) + \overline{v_{x0}}}{1 + Ct\left(\overline{\overline{U_x}} - \overline{v_{x0}}\right)}. \quad (23)$$

I now average equation (23) over the hop duration (equation (20)) to obtain the average horizontal particle speed as

$$\overline{\overline{v_x}} = \overline{\overline{U_x}} - \frac{1}{C\overline{t_{hop}}}\ln\left[1 + C\overline{t_{hop}}\left(\overline{\overline{U_x}} - \overline{v_{x0}}\right)\right]. \quad (24)$$

3. Results

[17] I obtain the impact threshold from the analytical model by iteratively solving equations (3)–(8), (13), (15)–(17), (20), (21), and (24). The result of this procedure is plotted in Figure 2a for Earth ambient conditions (as used by *Kok and Renno* [2009b]) and is compared with measurements of the impact threshold and simulations with COMSALT. The analytical model approximately reproduces the measurements, although the averaging procedures it employs result in a somewhat less accurate solution than the stochastic simulations of COMSALT. For Mars conditions (as used by *Kok* [2010]), the impact threshold is approximately an order of magnitude below the fluid threshold (Figure 2b). This result is quantitatively consistent with *Kok* [2010], and qualitatively consistent with *Claudin and Andreotti* [2006] and *Almeida et al.* [2008].

[18] Since the impact threshold lies below the fluid threshold on both Earth and Mars, hysteresis occurs on both planets. That is, saltation occurs between the impact and fluid thresholds if the wind speed exceeded the fluid threshold more recently than that it dropped below the impact threshold [*Kok*, 2010]. Figure 3 uses equation (1) and the analytical computation of the impact threshold to quantify this effect by computing the probability that saltation takes place at any given moment (or, equivalently, the average fraction of time that saltation takes place over a given time period) for a given mean shear velocity. For Earth conditions, equation (1) approximately reproduces measurements of the saltation probability by *Rasmussen and Sørensen* [1999]. Although hysteresis results in only a small increase in the saltation probability on Earth (Figure 3a), the much smaller ratio of the impact and fluid thresholds on

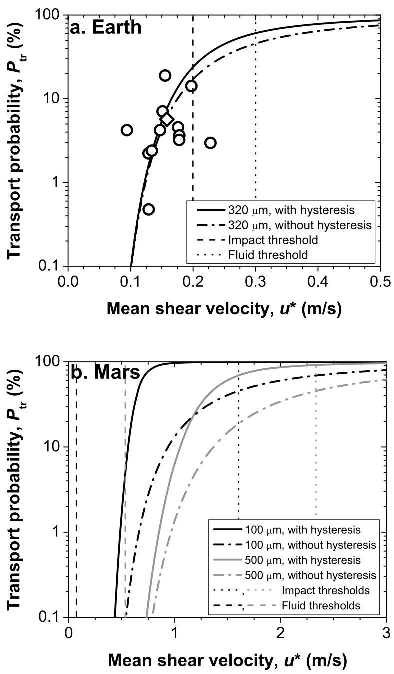

Figure 3. The probability P_{tr} that saltation transport occurs as a function of the mean shear velocity. Solid lines include the effect of hysteresis and were calculated from equation (1), whereas dash-dotted lines do not include the effect of hysteresis and represent the fraction of time that the wind exceeds the fluid threshold (i.e., the first term on the right-hand side in equation (1)); both calculations use $k = 2$ [*Kok*, 2010]. The fluid threshold (dotted vertical lines) was taken from the measurements of *Rasmussen and Sørensen* [1999] for (a) Earth conditions, and from *Greeley and Iversen* [1985] for (b) Mars conditions; the impact threshold (dashed vertical lines) was obtained using the analytical model. The calculations for Earth conditions are for 320 μm particles and are compared to measurements of the fraction of time saltation occurred during ~40 minute intervals in a field experiment (circles [*Rasmussen and Sørensen*, 1999]), as well as the average over all those measurements (diamond). Calculations for Mars conditions are for both 100 (black lines) and 500 μm (grey lines) particles. The relative error in P_{tr} due to the uncertainty in u^*_{it} (see Text S2) varies greatly with u^* but reaches a maximum of ~40% when $P_{tr} \approx 10\%$. Note that uncertainties in the exact value of the shape factor k [*Seguro and Lambert*, 2000] produce much greater uncertainties in P_{tr}.

Mars allows sand transport there to take place for a substantial fraction of time at mean shear velocities well below the fluid threshold (Figure 3b). As discussed by *Kok* [2010], this phenomenon has important implications for the formation of dunes, ripples, and possibly dust storms.

[19] To facilitate a simple calculation of the impact threshold in future studies, I curve fit the result of the analytical model, and obtain

$$u^*_{it} = c_1 \left(\frac{700}{P}\right)^{\frac{1}{6}} \left(\frac{220}{T}\right)^{\frac{2}{5}} \exp\left[\left(c_2/D_p\right)^3 + c_3\sqrt{D_p} - c_4 D_p\right], \quad (25)$$

with $c_1 = 5.5 \times 10^{-3}$ m/s, $c_2 = 49\ \mu$m, $c_3 = 0.29\ \mu\text{m}^{-1/2}$, and $c_4 = 3.84 \times 10^{-3}\ \mu\text{m}^{-1}$. Equation (25) has a difference from the analytical result of ~0.2–8% within the range P = 500–1000 Pa, T = 180–270 K, and D_p = 50–1000 μm. I furthermore quantify the effect of hysteresis on the height-integrated saltation mass flux Q by including it into White's mass flux equation [*White*, 1979], and obtain

$$Q = P_{tr} C_Q \frac{\rho_a}{g} (u^* - u^*_{it})(u^* + u^*_{it})^2, \quad (26)$$

where the transport probability P_{tr} is defined in equation (1), and $C_Q \approx 2.61$ is a proportionality constant that is tuned to match measurements [*White*, 1979].

4. Discussion and Conclusions

[20] The main results of the present study are the quantification of the Martian impact threshold (equation (25)) and the saltation mass flux equation accounting for the effect of hysteresis (equation (26)). Since both equations were derived using theory and numerical modeling, they should be tested with wind tunnel experiments under Martian conditions. However, because of the low fluid density on Mars, saltation there takes a much greater distance to reach steady state than on Earth. In fact, the "drag length" required to accelerate particles to the fluid speed is approximately two orders of magnitude greater on Mars than on Earth [*Kroy et al.*, 2005]. Since wind tunnels require ~10 meters to reach steady-state saltation for Earth conditions [*Shao and Raupach*, 1992], studies using similar wind tunnels for Mars conditions cannot measure steady-state conditions, and will thus underestimate the mass flux [*Anderson and Haff*, 1991; *Shao and Raupach*, 1992]. However, a measurement that can be made is to feed sand particles into the flow at speeds close to the steady-state impact speed (equation (13)) and vary the wind speed around the predicted impact threshold. Measurements of the resulting mass flux can then be used to check the accuracy of equations (25) and (26).

[21] Equations (25) and (26) could also be used to predict the saltation flux that leads to dust emission [*Greeley and Iversen*, 1985]. Note that this should be done with caution, since the addition of non-erodible elements (e.g., rocks), dust deposits, and induration (cementation) of the soil surface will likely affect the impact threshold. Further research is required to settle these questions.

[22] **Acknowledgments.** The author thanks Samuel Levis and Tom Warner for comments on the manuscript. The National Center for Atmospheric Research (NCAR) is sponsored by the National Science Foundation.

References

Almeida, M. P., et al. (2008), Giant saltation on Mars, *Proc. Natl. Acad. Sci. U. S. A.*, *105*(17), 6222–6226, doi:10.1073/pnas.0800202105.
Anderson, R. S., and P. K. Haff (1991), Wind modification and bed response during saltation of sand in air, *Acta Mech.*, *1*, 21–51.
Bagnold, R. A. (1937), The transport of sand by wind, *Geogr. J.*, *89*(5), 409–438, doi:10.2307/1786411.
Bagnold, R. A. (1941), *The Physics of Blown Sand and Desert Dunes*, Methuen, New York.
Claudin, P., and B. Andreotti (2006), A scaling law for aeolian dunes on Mars, Venus, Earth, and for subaqueous ripples, *Earth Planet. Sci. Lett.*, *252*(1–2), 30–44, doi:10.1016/j.epsl.2006.09.004.
Crane Company (1988), Flow of fluids through valves, fittings, and pipe, *Tech. Pap. 410*, Lacey, Wash.

Creyssels, M., et al. (2009), Saltating particles in a turbulent boundary layer: Experiment and theory, *J. Fluid Mech.*, *625*, 47–74, doi:10.1017/S0022112008005491.

Greeley, R., and J. D. Iversen (1985), *Wind as a Geological Process on Earth, Mars, Venus, and Titan*, doi:10.1017/CBO9780511573071, Cambridge Univ. Press, New York.

Iversen, J. D., and K. R. Rasmussen (1994), The effect of surface slope on saltation threshold, *Sedimentology*, *41*(4), 721–728, doi:10.1111/j.1365-3091.1994.tb01419.x.

Kok, J. F. (2010), Difference in wind speeds required for initiation versus continuation of sand transport on Mars: Implications for dunes and dust storms, *Phys. Rev. Lett.*, *104*, 074502, doi:10.1103/PhysRevLett.104.074502.

Kok, J. F., and N. O. Renno (2008), Electrostatics in wind-blown sand, *Phys. Rev. Lett.*, *100*, 014501, doi:10.1103/PhysRevLett.100.014501.

Kok, J. F., and N. O. Renno (2009a), The electrification of wind-blown sand on Mars and its implications for atmospheric chemistry, *Geophys. Res. Lett.*, *36*, L05202, doi:10.1029/2008GL036691.

Kok, J. F., and N. O. Renno (2009b), A comprehensive numerical model of steady state saltation (COMSALT), *J. Geophys. Res.*, *114*, D17204, doi:10.1029/2009JD011702.

Kroy, K., S. Fischer, and B. Obermayer (2005), The shape of barchans dunes, *J. Phys. Condens. Matter*, *17*, S1229, doi:10.1088/0953-8984/17/14/012.

Leovy, C. (2001), Weather and climate on Mars, *Nature*, *412*, 245–249, doi:10.1038/35084192.

Rasmussen, K. R., and M. Sørensen (1999), Aeolian mass transport near the saltation threshold, *Earth Surf. Processes Landforms*, *24*, 413–422, doi:10.1002/(SICI)1096-9837(199905)24:5<413::AID-ESP997>3.0.CO;2-I.

Rasmussen, K. R., and M. Sørensen (2008), Vertical variation of particle speed and flux density in aeolian saltation: Measurement and modeling, *J. Geophys. Res.*, *113*, F02S12, doi:10.1029/2007JF000774.

Rice, M. A., et al. (1995), An experimental study of multiple grain-size ejecta produced by collisions of saltating grains with a flat bed, *Sedimentology*, *42*(4), 695–706, doi:10.1111/j.1365-3091.1995.tb00401.x.

Ruf, C., et al. (2009), Emission of non-thermal microwave radiation by a Martian dust storm, *Geophys. Res. Lett.*, *36*, L13202, doi:10.1029/2009GL038715.

Seguro, J. V., and T. W. Lambert (2000), Modern estimation of the parameters of the Weibull wind speed distribution for wind energy analysis, *J. Wind Eng. Ind. Aerodyn.*, *85*, 75–84, doi:10.1016/S0167-6105(99)00122-1.

Shao, Y., and M. R. Raupach (1992), The overshoot and equilibration of saltation, *J. Geophys. Res.*, *97*(D18), 20,559–20,564.

White, B. R. (1979), Soil transport by winds on Mars, *J. Geophys. Res.*, *84*(B9), 4643–4651, doi:10.1029/JB084iB09p04643.

Wu, C. C., and A. N. L. Chiu (1983), Comparison of some ambient and typhoon instantaneous wind-speed characteristics, *J. Wind Eng. Ind. Aerodyn.*, *13*, 43–53, doi:10.1016/0167-6105(83)90127-7.

J. F. Kok, Advanced Study Program, National Center for Atmospheric Research, PO Box 3000, Boulder, CO 80307, USA. (jfkok@umich.edu)